

# Zinc Oxide Nanoparticles: A Comparative Study of Structural and Optical Properties of Green and Chemically Synthesized Nanoparticles

Pooja Choudhary<sup>1</sup>, Dinesh Arora<sup>1</sup>, Vishwajit Hooda<sup>1</sup>, Sunder Singh Arya<sup>2</sup> and Sunil Kumar<sup>1\*</sup>

<sup>1</sup>Department of Environmental Science, Maharshi Dayanand University, Rohtak 124 001, Haryana, India

<sup>2</sup>Department of Botany, Maharshi Dayanand University, Rohtak 124 001, Haryana, India

(Received 23 July, 2025; Accepted 17 September, 2025)

## ABSTRACT

Zinc oxide nanoparticles have garnered considerable attention for their unique properties and diverse applications in medicine, agriculture, and the environment. This study aims to assess the structural and optical properties of Zinc oxide nanoparticles synthesized by green and chemical methods using Banana peel extract and zinc acetate as precursors. Zinc oxide nanoparticles were synthesized using the co-precipitation method. Nanoparticles were characterized using zeta potential, UV-Visible spectroscopy, Fourier Transform Infrared Spectroscopy, Scanning Electron Microscopy, Energy-Dispersive X-ray analysis, and X-ray diffraction. UV-vis spectra showed absorption peaks at ~347 nm (green) and ~356 nm (chemical), indicating high excitation binding energy. Fourier Transform Infrared Spectroscopy confirmed the presence of Zn-O stretching and vibration, while Scanning Electron Microscopy revealed distinct nanorod and nanosphere morphologies. The green-synthesized nanoparticles ranged from 34–59 nm, whereas the chemically synthesized ones measured 13–50 nm. Energy-dispersive X-ray analysis confirmed high elemental purity, and X-ray diffraction demonstrated a hexagonal wurtzite crystalline structure for both samples. Chemically synthesized Zinc oxide nanoparticles offer greater uniformity for applications requiring precise and consistent particle characteristics, while green synthesis is eco-friendly, reducing energy use and minimizing by-product formation, thereby promoting environmentally sustainable practices. The findings of this study demonstrate an eco-friendly approach for the synthesis of zinc oxide nanoparticles, facilitating their potential application in sustainable industrial and biomedical practices.

**Key words:** Zinc oxide Nanoparticles, Green synthesis, Chemical synthesis, Banana peel.

## Introduction

Nanotechnology, which uses artificially or naturally produced particles known as nanoparticles (NPs), is the study of creating and using “petite” particles with  $10^{-9}$ m diameters. Their properties include higher strength, less weight, improved electrical conductivity, alteration of chemical reactivity, small

size, and a huge surface area-to-volume ratio (Shamhari *et al.*, 2018). They also exhibit enhanced reactivity, strength, and electrical characteristics. Environmental contaminants like organic pollutants are remediated from water and soil using NPs (Shivangi, 2023). NPs’ strong reactivity and enormous surface area make them very effective catalysts. They are employed in a number of industrial

operations to save costs and improve reaction efficiency (Boopathi and Davim, 2023).

Zinc and its oxide are among the most intriguing and promising metallic NPs. Zinc oxide nanoparticles (ZnPs) are versatile semiconductors that exhibit notable optical transparency and luminous capabilities. Because of their superior chemical and thermal durability, these NPs have gained importance in recent years (Cao *et al.*, 2011). Zinc is a strong reducing agent, and it can readily oxidize to generate zinc oxide based on its reduction potential (Król *et al.*, 2017). According to Dušan and Petar (2010), ZnPs have several benefits, including low cost, antibacterial activity, photocatalytic potential, and the ability to create structures with intriguing optical characteristics. According to Sani *et al.* (2023), ZnPs find use in a number of industries, like rubber, photocatalysis, pharmaceuticals, textiles, and electrotechnology. Various methods for the synthesis of ZnPs have been developed, such as hydrothermal, spray pyrolysis, sol-gel, chemical vapor deposition, precipitation methods, and ultrasonic conditions (Lu and Yeh, 2000; Okuyama and Lenggoro, 2003; Zak *et al.*, 2011; Omri *et al.*, 2014).

Extensive studies have been conducted on the chemical synthesis of ZnPs utilizing various approaches, and their utilization due to their high luminous efficiency, wide bandgap (3.36 eV), and substantial exciton binding energy (60 meV) (Król *et al.*, 2017). Despite these benefits, NPs have drawbacks, especially their possible toxicity and environmental impact.

On the other hand, biological approaches are increasingly being used since they are frequently safe, inexpensive, and clean. Additionally, the NPs made from plant extracts are more stable, and the plants are readily safe to handle (Chikkanna *et al.*, 2018). An environmentally friendly and economical way to create ZnPs is by green synthesis, which uses plant extracts. For example, pomegranate, beetroot, and spinach extracts produced ZnPs with particle sizes ranging from 20 to 30 nm (Mousa *et al.*, 2024). Similarly, ZnPs made with aloe vera demonstrated their promise for photocatalytic applications with a bandgap of 4.37 eV and a particle size of 5.86 nm (Singh and Jain, 2024).

The current study initially outlines the synthesis of ZnPs utilizing chemical and green methods. For green synthesis, banana peel was used. The banana, or *Musa paradisiaca*, is a member of the Musaceae family. It grows in the warm and humid tropics. It

contains a high concentration of potassium, linoleic acid, sterol fatty acid, fructose, glucose, xylose, and mannose, as well as some phenolic compounds (Imam and Akter, 2011). Several of these compounds can act as reducing agents and catalysts during the oxidation-reduction process by providing electrons to metal ions, which ultimately causes the ions to transform into the desired NPs (Miri *et al.*, 2021). In the chemical co-precipitation method, zinc acetate and NaOH were used. In this work, banana peel extracts were employed to determine the effectiveness of banana peels in creating NPs. The structural and optical properties of the synthesized ZnPs have been confirmed by zeta potential, UV-Visible spectroscopy, Fourier Transform Infrared Spectroscopy (FTIR), Scanning Electron Microscopy (SEM), Energy-Dispersive X-ray analysis (EDX), and X-ray diffraction (XRD) techniques.

## Materials and Methodology

### Chemicals

Zinc acetate ( $\text{Zn}(\text{OAc})_2 \cdot 2\text{H}_2\text{O}$ ), sodium hydroxide (NaOH), and an aqueous extract of banana peel were utilized in the experiment. All chemicals employed were of analytical reagent grade, and solutions were prepared using deionized water (DW).

### Preparation of banana peel aqueous extract

*Musa Paradisiaca*, the Banana, was purchased from the Rohtak market. The peels were collected, washed with DW, and left to dry in the oven overnight. The dried peels were then ground into a powder using a mortar and pestle, combined with 300 ml of deionized water, and heated for 30 minutes at 700 °C with a heater stirrer. After removing the residue with a centrifuge set to 6000 rpm for 20 minutes, the mixture was filtered through Whatman filter paper and stored for later use.

### Green synthesis of ZnPs

ZnPs were prepared by the co-precipitation method (Dadalioglu and Evrendilek, 2004). To synthesize ZnPs by  $\text{Zn}(\text{OAc})_2 \cdot 2\text{H}_2\text{O}$  and the banana peel extract, 50 ml of 0.02M  $\text{Zn}(\text{OAc})_2 \cdot 2\text{H}_2\text{O}$  was combined with 10mL of the banana peel aqueous extract, and the resulting mixture was stirred at room temperature with a magnetic stirrer for 2 to 3 hours until a precipitate with an off-white colour was obtained. The residue was washed several times in DW, fol-

lowed by ethanol to remove impurities. The final product was a white precipitate dried overnight in an oven at 55 °C. The powder was placed in a crucible and calcinated at 350-400 °C for 3 hrs in a muffle furnace. Complete conversion of Zn(OH)<sub>2</sub> into ZnO occurred during drying. Finally, the material was ground using a mortar pestle and stored in an airtight container.

### Chemical synthesis of ZnPs

To the aqueous zinc acetate solution, NaOH solution was added gradually, dropwise under vigorous stirring, and stirring was maintained for an additional 3-4 hours. The resulting precipitate was then filtered and carefully washed 3 times with DW, followed by ethanol to remove impurities. The final product was a milky white precipitate, which was dried overnight at 60 °C in an oven. The dried material was placed in a crucible and calcinated at 450 °C for 3-4 hours in a muffle furnace. Finally, the material was ground to a fine powder and stored in a container.

### Characterization of ZnPs

Several methods were used to characterize the synthesized ZnPs. After the completion of the reaction, 1-2 ml of the suspension was taken from the purified sample for the zeta (zetasizer Nano-ZS) and UV-Vis analysis (UV-3600 plus). An FTIR spectrometer (Perkin Elmer) was used to examine the chemical

composition. Scanning electron microscopy (Quorum, Q150ES plus) was used to study the nanoparticles' size and shape. Using a diffractometer, XRD (SmartLab 3kW) analysis was used to assess the phase purity and grain size. EDX (Quorum, Q150ES plus) was used for the analysis of the elemental composition and purity.

## Results and Discussion

The study tracks colour changes to document the creation of NPs when exposed to banana peel extract. The result of synthesis I (green synthesis) was a pale white precipitate, while synthesis II (chemical synthesis) produced a white precipitate.

### Zeta Potential

The surface charges that ZnPs gained were detected via zeta potential analysis. There won't be any NP aggregation if the particles in a suspension have high zeta potential (positive and negative). In Figure 1, both samples show negative zeta potential values of -26.7 mV (A) and -28 mV (B), which indicates good colloidal stability since particles with zeta potential above ±30 mV are generally considered stable due to electrostatic repulsion. ZnPs produced by various techniques in previous studies have zeta potentials ranging from -10.1 mV to -51.8 mV, which suggests moderate to high stability in colloidal solu-

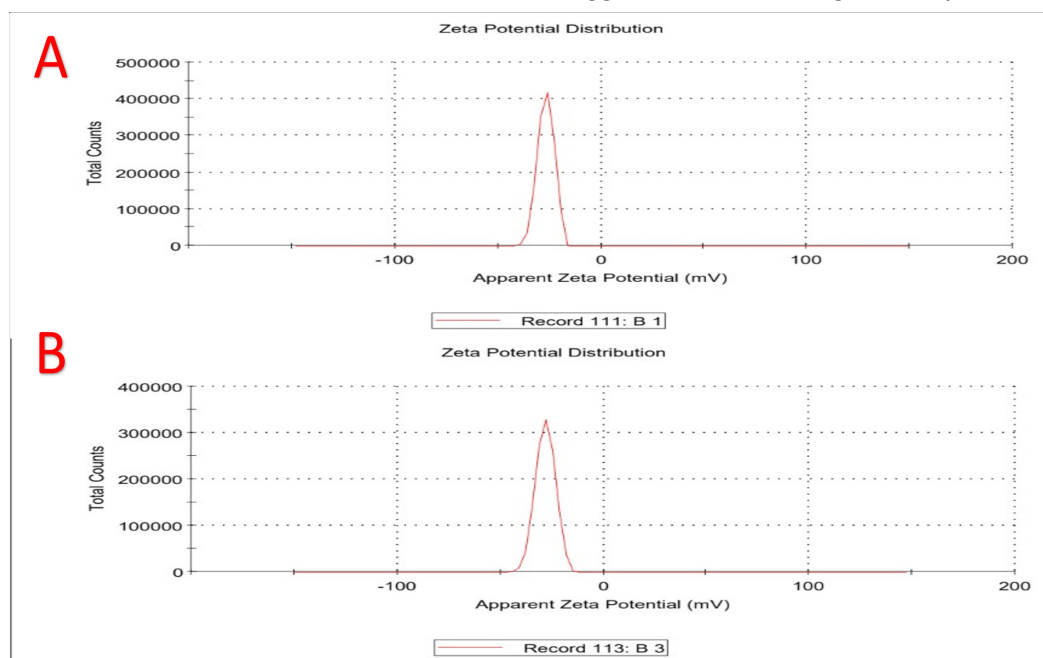


Fig. 1. Zeta potential of the ZnPs by (A) green synthesis and (B) chemical synthesis.

tions (Hamdy *et al.*, 2023; Abdullah *et al.*, 2024; Casiano-Muñiz *et al.*, 2024). In Abdullah *et al.* (2024) and Hamdy *et al.* (2023) experiments, zeta potential values for biosynthesized ZnPs ranged from -20.4 mV to -46.7 mV, indicating low aggregation and strong stability.

### UV-Visible spectroscopy

NPs are characterized using UV-visible spectroscopy to determine their optical properties and maximum absorbance. Figure 2 shows the UV-visible absorption spectrum of the produced NPs. There is an absorption peak at 346 nm in Spectrum A and a peak at 356 nm in Spectrum B. There are physical variations between the chemically produced and green NPs, probably related to surface features or particle size, as evidenced by the 10 nm shift in peak location. A similar result of an absorption band at 355 that represents ZnPs was also obtained from these peaks by Talam *et al.* (2012). Absorption spectroscopy demonstrated that when the size of NPs decreases, the band gap widens. The absorption wavelength and band gap likewise have an opposing ratio. Previous studies proved that ZnPs absorb at a wavelength of approximately 385 nm (Ogunyemi *et al.*, 2019; Jayappa *et al.*, 2020; Almoneef *et al.*, 2024). According to Jayappa *et al.* (2020), ZnPs' absorption maxima were seen in the UV range between 350 and 380 nm, which corresponds to band gap energies between 3.1 and 3.54 eV.

### FTIR

FTIR spectroscopy analysis of the synthesized ZnPs is presented in Figure 3. FTIR was employed to verify the purity of the NPs and to detect the presence of phyto-chemicals. The chemically synthe-

sized sample exhibits a cleaner spectrum with fewer organic-related peaks. In contrast, the green synthesis sample shows a more complex organic signature, due to the presence of phytochemicals from the extract, which act as both reducing and capping agents. The green synthesis, using banana peel extract, exhibited a complex organic signature with several characteristic peaks. A broad peak at 3477.71  $\text{cm}^{-1}$  indicated O-H stretching from water and hydroxyl groups, while peaks at 2354.36 and 2312.77  $\text{cm}^{-1}$  were attributed to atmospheric  $\text{CO}_2$  or CN stretching from nitrogen-containing compounds (Fakhari *et al.*, 2019). Notably, the most intense peak at 1454.96  $\text{cm}^{-1}$  was due to C-H bending, or nitrate bending, suggesting significant incorporation of organic compounds. Zn-O stretching vibrations were confirmed by peaks at 844.69, 761.25, 696.83, 667.48, and 499.10  $\text{cm}^{-1}$  (Agarwal *et al.*, 2017). In biosynthesized ZnPs, additional peaks that corresponded to organic functional groups, including C-H, C-N, and C=O, were detected, suggesting the presence of capping agents derived from plant extracts (Ullah *et al.*, 2024).

In contrast, the chemically synthesized ZnPs using zinc acetate showed a much cleaner spectrum with fewer organic-related peaks, indicating greater purity and minimal surface functionalization. A broad peak at 3439.68  $\text{cm}^{-1}$  and a peak at 1626.16  $\text{cm}^{-1}$  were associated with O-H stretching and bending from adsorbed water. Peaks at 1409.04 and 1115.35  $\text{cm}^{-1}$  were due to residual acetate groups (Jayachandran *et al.*, 2021). Strong Zn-O stretching vibrations appeared at 690.06 and 563.20  $\text{cm}^{-1}$ , while a cluster of intense peaks in the 400–450  $\text{cm}^{-1}$  range confirmed high crystallinity and well-defined ZnO structures (Gur *et al.*, 2022). Overall, the green synthesis produced bio-functionalized ZnPs, while

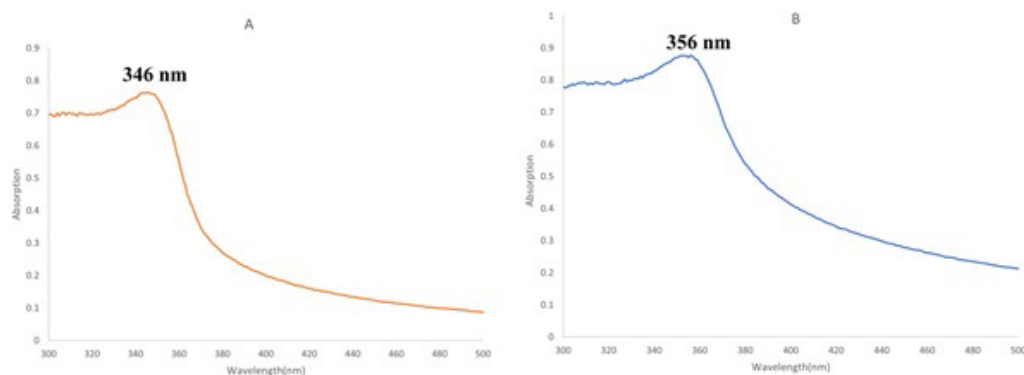


Fig. 2. UV-visible spectrum of the ZnPs by (A) green synthesis and (B) chemical synthesis.

chemical synthesis resulted in highly crystalline and purer NPs. The hydroxyl groups (about 3200-3500  $\text{cm}^{-1}$ ) and Zn-O stretching vibrations (approximately 450-500  $\text{cm}^{-1}$ ) were usually represented by absorption bands in ZnPs FTIR spectra (Almoneef *et al.*, 2024).

**SEM**

SEM analyses determine the size and structure of the produced ZnPs. Micrographs of ZnPs demonstrated their homogeneous distribution, spherical

shape, and range of nanosizes. In Figure 4(A), the green synthesis shows particle sizes ranging from 34 to 59nm, and in Figure 4(B), the chemical synthesis shows particle sizes ranging from 13 to 50 nm. The chemically synthesized NPs appear to have a more uniform size distribution and smoother morphology, while the green-synthesized particles show greater variation in size and surface characteristics. Madan *et al.* (2013) have already described a similar homogenous spherical shape of ZnPs. The structural differences between these samples indicate that the

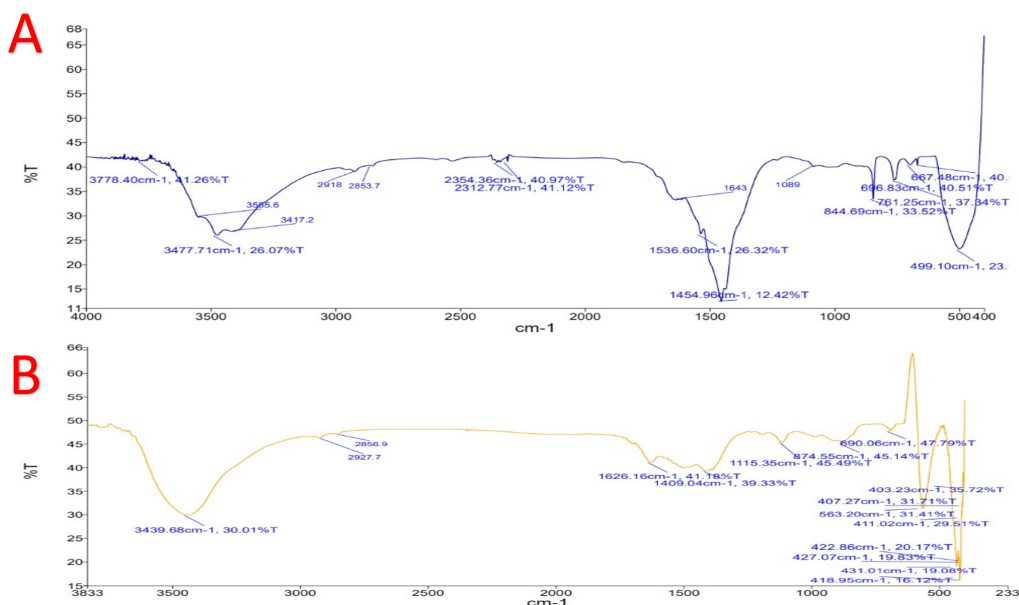


Fig. 3. FTIR analysis of the ZnPs by (A) green synthesis and (B) chemical synthesis.

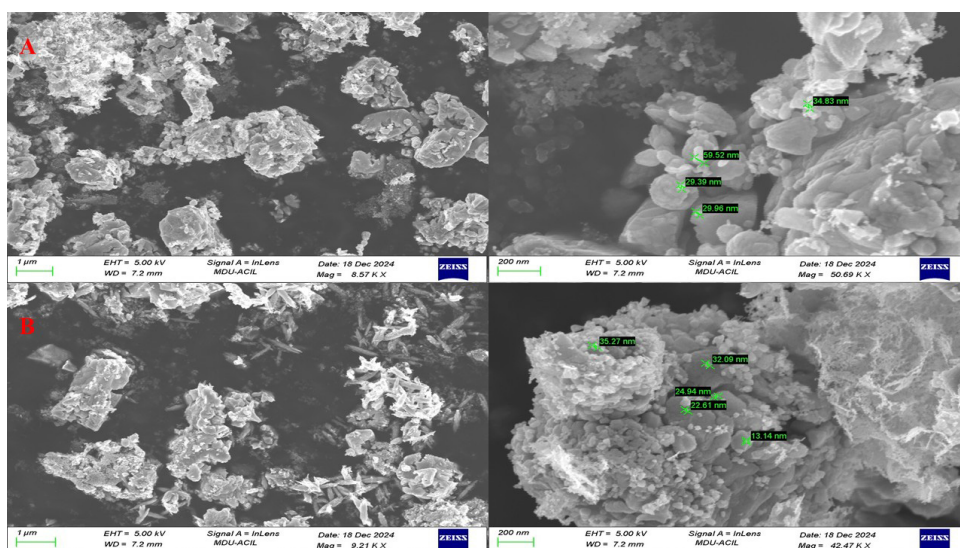


Fig. 4. SEM micrographs of ZnPs (A) green synthesis and (B) chemical synthesis.

synthesis method significantly influences the final particle characteristics, which could have important implications for their potential applications. In previous studies, the morphologies of ZnPs produced by various techniques included spherical, irregular, and agglomerated shapes (Hamdy *et al.*, 2023; Flemban, 2023). Depending on the synthesis process and variables like temperature, concentration, and reaction time, the ZnPs size varied from 5-100 nm (Sharma *et al.*, 2024).

**EDX spectroscopy**

The elemental makeup of the ZnPs, as determined from the EDX analysis of the SEM images shown in Figure 5, indicated the presence of Zn and O in the samples. The EDX spectra confirmed that the synthesized ZnPs possessed high purity and contained the desired Zn and O phases. The elemental analysis of the NPs revealed a composition of 66.8% zinc and 28.6% oxygen for green synthesis and 68.7% zinc and 28.3% oxygen for chemical synthesis, confirming that the synthesized NPs were of exceptionally high purity. Sample B shows higher peak intensities than Sample A, with its primary zinc peak reaching about 3.60K counts as opposed to Sample A's 2.07K counts. This intensity difference may result from variations in sample thickness or density rather than true concentration differences. These

findings align closely with those reported in previous studies. The successful synthesis of high-purity NPs was confirmed by the elemental composition, which matched the anticipated stoichiometry of ZnO (Almoneef *et al.*, 2024; Merdan and Banimuslem, 2024).

**XRD**

The XRD analysis of ZnPs in figure 6 (green and chemical synthesis) exhibited distinct peaks at various scattering angles ( $2\theta$ ) of 31.9 and 31.72, 34.58 and 34.38, 36.32 and 36.24, 47.62 and 47.5, 56.76 and 56.58, 62.88 and 62.82, 68.08 and 67.94, corresponding to reflection from the 100, 002, 101, 102, 110, 103 and 112 diffraction lattice planes respectively. Both patterns display characteristic peaks of the hexagonal wurtzite structure of ZnPs, which is the most stable crystalline form of ZnPs at ambient conditions. The peaks of the synthesized ZnPs were in close agreement with the previous findings (Flemban, 2023; Hamdy *et al.*, 2023). The highest intensity peak at around 36.32-36.24 in both patterns corresponds to the (101) plane of the wurtzite ZnO structure. These peaks are consistent with those reported by Kotresh *et al.* (2021). The similarities between the two patterns suggest that both synthesis methods (green and chemical) produced ZnPs with similar crystalline structures. However, there are

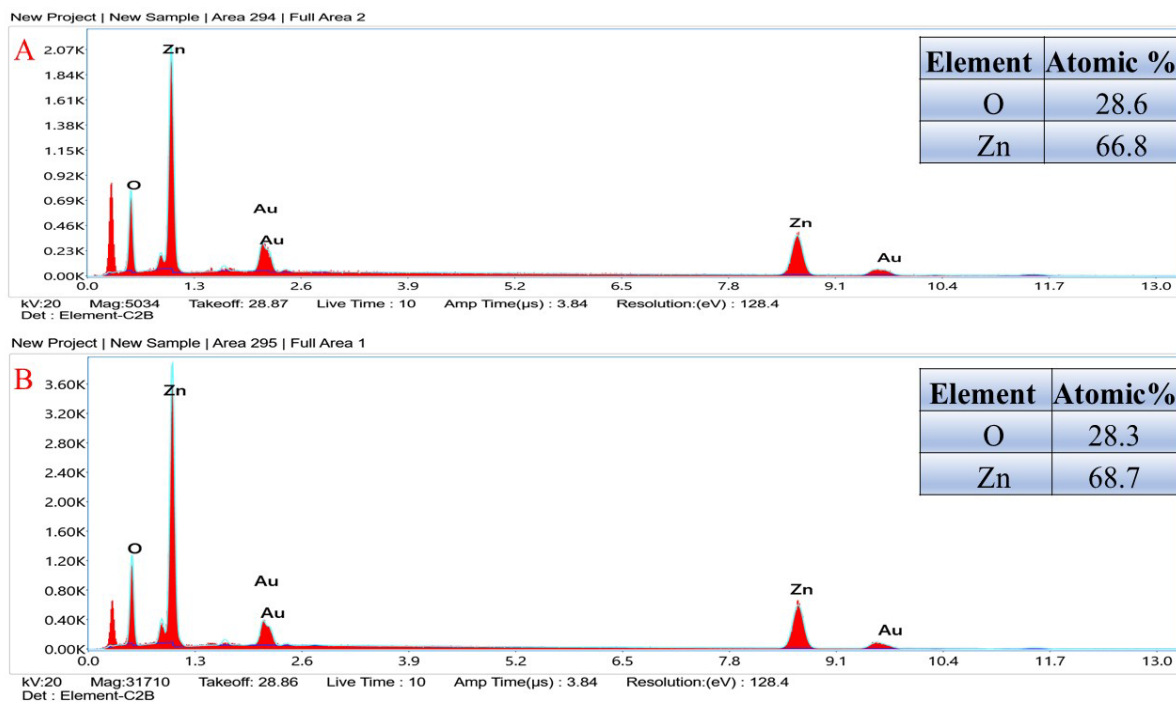


Fig. 5. EDX analyses of ZnPs (A) green synthesis and (B) chemical synthesis.

slight differences in peak positions and relative intensities, which might indicate minor variations in crystallite size, strain, or possible impurities between the two synthesis methods (Arumugam *et al.*, 2021).

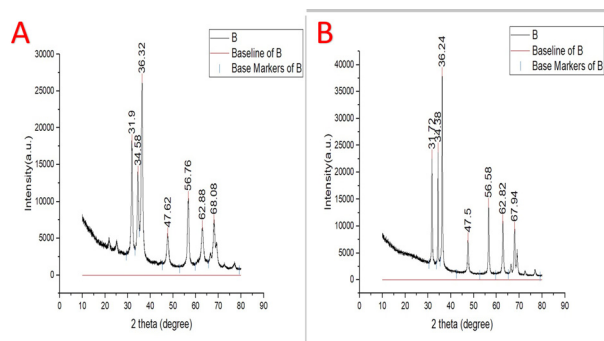


Fig. 6. XRD analyses of ZnPs (A) green synthesis and (B) chemical synthesis.

### Comparative analysis of synthesized ZnPs

Table 1 provides a comparative overview of the various plant species employed in the green synthesis of ZnPs, along with their characterization, in relation to the present study. The size of the ZnPs in previous studies ranges from 20 to 87nm, while the present study shows the range from 34 to 56nm in green synthesis. Table 2 shows the results of ZnPs characterizations from previous studies in comparison with the present study.

### Conclusion

This research successfully synthesized ZnPs using green and chemical methods. The results highlight the advantages of green synthesis, which aligns with sustainable nanotechnology principles. The green synthesis yielded bio-functionalized ZnPs with distinct organic signatures and slightly larger, more varied particle sizes, while chemical synthesis yields purer, highly crystalline, and uniform NPs. Both methods displayed good colloidal stability, as shown by zeta potential. UV-Vis spectra revealed characteristic absorption peaks influenced by particle size, and FTIR analyses confirmed the role of phenolic and carboxylic acid groups in NPs formation. SEM analysis highlights the distinct nanorod and nanosphere morphologies, and EDX confirms the elemental purity, and XRD verifies the hexagonal wurtzite structure of ZnPs. Particle size strongly affects application; smaller ZnPs (1-50 nm) suit high-

Table 1. Different plants used for the green synthesis of ZnPs

Plants	Size	UV-Visible	SEM	XRD	References
<i>Nyctanthesarbor-tristis</i> (Jasmine)	87.5nm	302 nm	Nanoscale and uniform	Crystalline	Kumar and Shrotriya (2024)
<i>Punica granatum</i> (Pomegranate)	20-30nm	295 nm	Nanoscale and uniform	Crystalline planes	Mousa <i>et al.</i> (2024)
<i>Tinospora cordifolia</i> (Giloy)	21 nm	374 nm	rectangular and triangular shapes	Crystalline nature	Jayaseelan <i>et al.</i> (2024)
<i>Pistia Stratiotes</i> (Water Lettuce)	35 nm	368 nm	spherical, flower, and sheet-like shapes	Crystalline nature	Meji <i>et al.</i> (2024)
<i>Malva neglecta</i> (Dwarf Mallow)	40-50 nm	368nm	spherical and hexagonal shapes	Crystalline nature	Cheperli <i>et al.</i> (2024)
<i>Bacopa monnieri</i> (Brahmi)	33-36 nm	366 nm	Hexagonal-shaped	Crystalline nature	Singh <i>et al.</i> (2023)
<i>Musa paradisiaca</i> (Banana)	34-59 nm	346 nm	nanosphere	Crystalline nature	Present Study

**Table 2.** Key findings of the different characterization of ZnPs from previous studies

Techniques	Key findings of previous studies	Findings of this study (green and chemical)	References
Zeta Potential	Values ranged from -10.1 mV to -51.8 mV, indicating moderate to high stability	Both samples show negative zeta potential values of -26.7 mV and -28 mV.	Hamdy <i>et al.</i> (2023); Abdullah <i>et al.</i> (2024); Casiano-Muñiz <i>et al.</i> (2024)
UV-Visible Spectroscopy FTIR	Absorption peaks between 350 nm and 380 nm, band gap 3.1-3.54 eV Zn-O stretching (450-500 cm <sup>-1</sup> ), O-H (3200-3500 cm <sup>-1</sup> ), and organic groups	Both samples show absorption peaks at 346 nm and 356 nm. Both samples show Zn-O stretching vibration peaks at 844.69, 761.25, 696.83, 667.48, 499.10 cm <sup>-1</sup> , and 690.06 and 563.20 cm <sup>-1</sup> .	Jayappa <i>et al.</i> (2020); Almoneef <i>et al.</i> (2024); Almoneef <i>et al.</i> (2024); Ullah <i>et al.</i> (2024)
SEM	Spherical, irregular, and agglomerated shapes; size range 5-100 nm	Both samples show particle sizes ranging from 34-59nm and 13-50 nm.	Hamdy <i>et al.</i> (2023); Flemban (2023); Sharma <i>et al.</i> (2024)
EDX	Primarily Zn and O, with minimal impurities	Both samples show a composition of 66.8% Zn and 28.6% O, and 68.7% Zn and 28.3% O.	Almoneef <i>et al.</i> (2024); Merdan and Banimuslem (2024)
XRD	Hexagonal wurtzite structure; crystallite size 5-34.27 nm	Both samples show the highest intensity peak at around 36.32-36.24, corresponding to the (101) plane of the wurtzite ZnO structure	Hamdy <i>et al.</i> (2023); Flemban, (2023)

reactivity uses like biomedicine and sensors, while larger ones (50–100 nm) are optimal for stable agricultural or industrial uses. Present research confirms that agricultural waste, such as banana peel, can be utilized for sustainable NPs synthesis, supporting further research into green approaches for industrial, medical, agricultural, and environmental applications where sustainability is crucial.

**Conflict of interest:** The authors declare that they have no conflict of interest.

**Funding:** Not applicable

## References

- Abdullah, J. A. A., Guerrero, A. and Romero, A. 2024. Efficient and Sustainable Synthesis of Zinc Salt-Dependent Polycrystal Zinc Oxide Nanoparticles: Comprehensive Assessment of Physicochemical and Functional Properties. *Applied Sciences*. <https://doi.org/10.3390/app14051815>
- Agarwal, H., Kumar, S.V. and Rajeshkumar, S. 2017. A review on green synthesis of zinc oxide nanoparticles—An eco-friendly approach. *Resource-Efficient Technologies*. 3(4): 406-413.
- Almoneef, M.M., Awad, M.A., Aldosari, H., Hendi, A. A., Aldehais, H. A., Merghani, N. M. and Alshammari, S.G. 2024. Exploring the multi-faceted potential: Synthesized ZnO nanostructure- Characterization, photo catalysis, and crucial biomedical applications. *Heliyon*. 10(12): e32714. <https://doi.org/10.1016/j.heliyon.2024.e32714>
- Arumugam, M., Manikandan, D.B., Dhandapani, E., Sridhar, A., Balakrishnan, K., Markandan, M. and Ramasamy, T. 2021. Green synthesis of zinc oxide nanoparticles (ZnPs) using *Syzygiumcumini*: Potential multifaceted applications on antioxidants, cytotoxic and as nano nutrient for the growth of *Sesamum indicum*. *Environmental Technology and Innovation*. 23: 101653. <https://doi.org/10.1016/J.ETI.2021.101653>
- Abisha Meji M, Usha, D. and Ashwin, B. M. 2024. Microwave-assisted green synthesis of zinc oxide nanoparticles using *pistia stratiotes* for anticancer and antibacterial applications. *Materials Research Express*. 11(8): 085004. <https://doi.org/10.1088/2053-1591/ad6d34>
- Boopathi, S. and Davim, J. P. 2023. *Applications of Nanoparticles in Various Manufacturing Processes* (pp. 1–31). IGI Global. <https://doi.org/10.4018/978-1-6684-9135-5.ch001>
- Cao, Y., Liu, B., Huang, R., Xia, Z. and Ge, S. 2011. Flash synthesis of flower-like ZnO nanostructures by microwave-induced combustion process. *Materials Letters*. 65(2): 160-163.
- Casiano-Muñiz, I.M., Ortiz-Román, M.I., Lorenzana-Vázquez, G. and Román-Velázquez, F. 2024. Synthe-

- sis, Characterization, and Ecotoxicology Assessment of Zinc Oxide Nanoparticles by *In vivo* Models. *Nanomaterials*. <https://doi.org/10.3390/nano14030255>
- Cheperli, A.M., Mokaber Esfahani, M., Taleghani, A. and Bahalkeh, F. 2024. Biosynthesis, characterization and antimicrobial activities of zinc oxide nanoparticles from leaf and seed extracts of *Malva neglecta* Wallr. *Inorganic and Nano-Metal Chemistry*. 1-11. <https://doi.org/10.1080/24701556.2024.2354923>
- Chikkanna, M.M., Neelagund, S.E. and Rajashekarappa, K. K. 2019. Green synthesis of zinc oxide nanoparticles (ZnPs) and their biological activity. *SN Applied Sciences*. 1(1): 117.
- Dadalioglu, I. and Evrendilek, G.A. 2004. Chemical compositions and antibacterial effects of essential oils of Turkish oregano, Bay Laurel, Spanish lavender, and fennel and common foodborne pathogens. *Journal of Agricultural and Food Chemistry*. 52(26): 8255-8260.
- Divya, M.J., Sowmia, C., Joon, K. and Dhanya, K.P. 2013. Synthesis of zinc oxide nanoparticle from Hibiscus rosa-sinensis leaf extract and investigation of its antimicrobial activity. *Research Journal of Pharmaceutical, Biological and Chemical Sciences*. 1137-1142.
- Dušan, N. and Petar, G. 2010. ZnO nanoparticles and their applications - new achievements. *Nanocon*. 1-6.
- Fakhari, S., Jamzad, M. and Kabiri Fard, H. 2019. Green synthesis of zinc oxide nanoparticles: a comparison. *Green Chemistry Letters and Reviews*. 12(1): 19-24.
- Flemban, T. H. 2023. Synthesis, characterization, and analysis of zinc oxide nanoparticles using varying pulsed laser ablation energies in liquid. *Journal of Experimental Nanoscience*. <https://doi.org/10.1080/17458080.2023.2175817>
- Gur, T., Meydan, I., Seckin, H., Bekmezci, M. and Sen, F. 2022. Green synthesis, characterization and bioactivity of biogenic zinc oxide nanoparticles. *Environmental Research*. 204: 111897.
- Hamdy, E., Al-Askar, A.A., El-Gendi, H., Khamis, W.M., Behiry, S.I., Valentini, F., Abd-Elsalam, K.A. and Abdelkhalek, A. 2023. Zinc Oxide Nanoparticles Biosynthesized by *Eriobotrya japonica* Leaf Extract: Characterization, Insecticidal and Antibacterial Properties. *Plants*. 12. <https://doi.org/10.3390/plants12152826>
- Imam, M.Z. and Akter, S. 2011. *Musa paradisiaca* L. and *Musa sapientum* L.: A phytochemical and pharmacological review. *Journal of Applied Pharmaceutical Science*. (Issue). 14-20.
- Jayachandran, A., Aswathy, T.R. and Nair, A.S. 2021. Green synthesis and characterization of zinc oxide nanoparticles using Cayratiaepedata leaf extract. *Biochemistry and Biophysics Reports*. 26: 100995.
- Jayappa, M.D., Jayappa, M.D., Ramaiah, C.K., Ramaiah, C.K., Pavan Kumar, M.A., Pavan Kumar, M.A., Suresh, D., Prabhu, A., Devasya, R.P., Sheikh, S. and Sheikh, S. 2020. Green synthesis of zinc oxide nanoparticles from the leaf, stem and in vitro grown callus of *Mussaenda frondosa* L.: characterization and their applications. *Applied Nanoscience*. 10(8): 1-18. <https://doi.org/10.1007/S13204-020-01382-2>
- Jayaseelan, C., Siva, D., Kamaraj, C., Thirugnanasambandam, R., Ganesh Kumar, V., Subashni, B., Ashokkumar, R. and Saravanan, D. 2024. Phytosynthesis of zinc oxide nanoparticles for enhanced antioxidant, antibacterial, and photocatalytic properties: A greener approach to environmental sustainability. *Environmental Research*. 118770. <https://doi.org/10.1016/j.envres.2024.118770>
- Kotresh, M.G., Patil, M.K. and Inamdar, S.R. 2021. Reaction temperature based synthesis of ZnO nanoparticles using co-precipitation method: Detailed structural and optical characterization. *Optik*. 243: 167506.
- Król, A., Pomastowski, P., Rafińska, K., Railean-Plugaru, V. and Buszewski, B. 2017. Zinc oxide nanoparticles: Synthesis, antiseptic activity and toxicity mechanism. *Advances in Colloid and Interface Science*. 249: 37-52.
- Kumar, A. and Shrotriya, A.K. 2024. Green Synthesis and Characterization of Zinc Oxide Nanoparticles Using *Nyctanthes arbor-tristis* Plant Extracts: Assessing Photocatalytic Properties. *International Journal for Science Technology And Engineering*. 12(7): 860-867. <https://doi.org/10.22214/ijraset.2024.63666>
- Lu, C.H. and Yeh, C. H. 2000. Influence of hydrothermal conditions on the morphology and particle size of zinc oxide powder. *Ceramics International*. 26(4): 351-357.
- Merdan, M. and Banimuslem, H. 2024. Synthesis, characterization and LDA+U calculations of zinc oxide nanoparticles. *Physica Scripta*. <https://doi.org/10.1088/1402-4896/ad4427>
- Miri, A., Beiki, H., Najafidoust, A., Khatami, M. and Sarani, M. 2021. Cerium oxide nanoparticles: green synthesis using Banana peel, cytotoxic effect, UV protection and their photocatalytic activity. *Bioprocess and Biosystems Engineering*. 44(9): 1891-1899.
- Mousa, S.A., wissa, dores, Hassan, H.H., Ebnalwaled, A.A. and Khairy, S.A. 2024. Enhanced photocatalytic activity of green synthesized zinc oxide nanoparticles using low-cost plant extracts. *Dental Science Reports*. 14(1). <https://doi.org/10.1038/s41598-024-66975-1>
- Ogunyemi, S.O., Abdallah, Y., Zhang, M., Fouad, H., Hong, X., Ibrahim, E. and Li, B. 2019. Green synthesis of zinc oxide nanoparticles using different plant extracts and their antibacterial activity against *Xanthomonas oryzae* pv. *oryzae*. *Artificial cells, Nanomedicine, and Biotechnology*. 47(1): 341-352.
- Okuyama, K. and Lenggoro, I.W. 2003. Preparation of

- nanoparticles via spray route. *Chemical Engineering Science*. 58(3-6): 537-547.
- Omri, K., Najeh, I., Dhahri, R., El Ghoul, J. and El Mir, L.J.M.E. 2014. Effects of temperature on the optical and electrical properties of ZnO nanoparticles synthesized by sol-gel method. *Microelectronic Engineering*. 128: 53-58.
- Sani, G.D., Yakubu, A., Saidu, A., Aati, R., Sahabi, S. and Abdullahi, S. 2023. A review on industrial applications of zinc oxide nanoparticles. *International Journal of Advances in Engineering and Management*. 5: 1031-1041.
- Shamhari, N.M., Wee, B.S., Chin, S.F. and Kok, K.Y. 2018. Synthesis and Characterization of Zinc Oxide Nanoparticles with Small Particle Size Distribution. *Acta Chimica Slovenica*. 65(3).
- Sharma, A., Kumar, P. and Mahapatra, S.P. 2024. Synthesis, Characterization, Dielectric, and Electrical Conductivity Studies of Zinc Oxide Nanoparticles. *IOP Conference Series: Materials Science and Engineering*. <https://doi.org/10.1088/1757-899x/1300/1/012025>
- Shivangi, M. 2023. Nanotechnology: an overview and its applications. In: *IIP Series Futuristic Trends in Chemical, Material Sciences & Nano Technology*. 98-112. <https://doi.org/10.58532/v2bs12p1ch7>
- Singh, P.P., Debnath, N., Bhatnagar, T., Das, S. and Chaturvedi, S. 2023. Comparative Evaluation of Biogenesis of ZnO Nanoparticles Using Leaf Extracts of *Bacopa monnieri*, *Acacia arabica* and *Catharanthus roseus*. *Indian Journal of Science and Technology*. <https://doi.org/10.17485/ijst/v16i37.2050>
- Singh, S. and Jain, B. 2024. Green synthesis of zinc oxide nanoparticles using aloe vera: a study on optical properties and photocatalytic activity. *Chem Rxiv*. <https://doi.org/10.26434/chemrxiv-2024-83hjj>
- Talam, S., Karumuri, S.R. and Gunnam, N. 2012. Synthesis, characterization, and spectroscopic properties of ZnO nanoparticles. *International Scholarly Research Notices*. 2012(1): 372505.
- Ullah, Z., Iqbal, J., Abbasi, B.H., Gul, F., Ijaz, S., Kanwal, S., Mahmoodi, M., Kazi, M. and Mahmood, T. 2024. *Rhynchosia capitata* driven bioproduction of Zinc oxide nanoparticles, characterization and multifaceted therapeutic applications. *Research Square*. <https://doi.org/10.21203/rs.3.rs-4442285/v1>
- Zak, A.K., Abrishami, M.E., Majid, W.A., Yousefi, R. and Hosseini, S.M. 2011. Effects of annealing temperature on some structural and optical properties of ZnO nanoparticles prepared by a modified sol-gel combustion method. *Ceramics International*. 37(1): 393-398.
-